

# Clinical and Magnetic Resonance Imaging Outcome Predictors in Pediatric Anti-N-Methyl-D-Aspartate Receptor Encephalitis

Frederik Bartels, MD <sup>1,2</sup> Stephan Krohn, MD,<sup>1,2</sup> Marc Nikolaus, MD,<sup>3,4</sup> Jessika Johannsen, MD,<sup>5</sup> Ronny Wickström, MD,<sup>6</sup> Mareike Schimmel, MD,<sup>7</sup> Martin Häusler, MD,<sup>8</sup> Andrea Berger, MD,<sup>9,10</sup> Markus Brey, MD,<sup>11</sup> Markus Blankenburg, MD,<sup>12,13</sup> Johannes Stoffels, MD,<sup>14</sup> Oliver Hendricks, MD,<sup>15</sup> Günther Bernert, MD,<sup>16</sup> Gerd Kurlemann, MD,<sup>17</sup> Ellen Knierim, MD,<sup>3,4</sup> Angela Kaindl, MD,<sup>3,4</sup> Kevin Rostásy, MD,<sup>13</sup> and Carsten Finke, MD <sup>1,2</sup>

**Objective:** To evaluate disease symptoms, and clinical and magnetic resonance imaging (MRI) findings and to perform longitudinal volumetric MRI analyses in a European multicenter cohort of pediatric anti-N-methyl-D-aspartate receptor encephalitis (NMDARE) patients.

**Methods:** We studied 38 children with NMDARE (median age = 12.9 years, range = 1–18) and a total of 82 MRI scans for volumetric MRI analyses compared to matched healthy controls. Mixed-effect models and brain volume z scores were applied to estimate longitudinal brain volume development. Ordinal logistic regression and ordinal mixed models were used to predict disease outcome and severity.

**Results:** Initial MRI scans showed abnormal findings in 15 of 38 (39.5%) patients, mostly white matter T2/fluid-attenuated inversion recovery hyperintensities. Volumetric MRI analyses revealed reductions of whole brain and gray matter as well as hippocampal and basal ganglia volumes in NMDARE children. Longitudinal mixed-effect models and z score transformation showed failure of age-expected brain growth in patients. Importantly, patients with abnormal MRI findings at onset were more likely to have poor outcome (Pediatric Cerebral Performance Category score > 1, incidence rate ratio = 3.50, 95% confidence interval [CI] = 1.31–9.31,  $p = 0.012$ ) compared to patients with normal MRI. Ordinal logistic regression models

View this article online at [wileyonlinelibrary.com](https://www.wileyonlinelibrary.com). DOI: 10.1002/ana.25754

Received Jul 12, 2019, and in revised form Apr 17, 2020. Accepted for publication Apr 18, 2020.

Address correspondence to Dr Finke, Department of Neurology, Charité–Universitätsmedizin Berlin, Charitéplatz 1, 10117 Berlin, Germany. E-mail: [carsten.finke@charite.de](mailto:carsten.finke@charite.de)

From the <sup>1</sup>Department of Neurology, Charité–Universitätsmedizin Berlin, Berlin, Germany; <sup>2</sup>Berlin School of Mind and Brain, Humboldt-Universität zu Berlin, Berlin, Germany; <sup>3</sup>Department of Pediatric Neurology, Charité–Universitätsmedizin Berlin, Berlin, Germany; <sup>4</sup>Center for Chronically Sick Children, Charité–Universitätsmedizin Berlin, Berlin, Germany; <sup>5</sup>Department of Pediatrics, University Medical Center Hamburg-Eppendorf, Hamburg, Germany; <sup>6</sup>Neuropediatric Unit, Karolinska University Hospital, Astrid Lindgren Children's Hospital, Stockholm, Sweden; <sup>7</sup>Department of Pediatric Neurology, University Children's Hospital Augsburg, Augsburg, Germany; <sup>8</sup>Department of Pediatrics, Division of Neuropediatric and Social Pediatrics, Medical University Rheinisch-Westfälische Technische Hochschule (RWTH) Aachen, Aachen, Germany; <sup>9</sup>Division of Pediatric Neurology, Department of Pediatrics, München Klinik Harlaching, Munich, Germany; <sup>10</sup>Division of Pediatric Neurology, Department of Pediatrics, Klinikum Weiden, Weiden, Germany; <sup>11</sup>Department of Pediatrics and Adolescent Medicine, Medical University of Vienna, Vienna, Austria; <sup>12</sup>Department of Pediatric Neurology, Olgahospital Stuttgart, Stuttgart, Germany; <sup>13</sup>Department of Pediatric Neurology, Children's Hospital Datteln, Witten/Herdecke University, Datteln, Germany; <sup>14</sup>Department of Pediatric Neurology, Children's Hospital Neuburg, Neuburg, Germany; <sup>15</sup>Department of Pediatrics, Marienhospital Bottrop, Bottrop, Germany; <sup>16</sup>Department of Pediatrics, Gottfried von Preyer's Children's Hospital, Vienna, Austria; and <sup>17</sup>Division of Pediatric Neurology, Department of Pediatrics, Medical University Münster, Münster, Germany

Additional supporting information can be found in the online version of this article.

corrected for time from onset confirmed abnormal MRI at onset (odds ratio [OR] = 9.90, 95% CI = 2.51–17.28,  $p = 0.009$ ), a presentation with sensorimotor deficits (OR = 13.71, 95% CI = 2.68–24.73,  $p = 0.015$ ), and a treatment delay > 4 weeks (OR = 5.15, 95% CI = 0.47–9.82,  $p = 0.031$ ) as independent predictors of poor clinical outcome.

**Interpretation:** Children with NMDARE exhibit significant brain volume loss and failure of age-expected brain growth. Abnormal MRI findings, a clinical presentation with sensorimotor deficits, and a treatment delay > 4 weeks are associated with worse clinical outcome. These characteristics represent promising prognostic biomarkers in pediatric NMDARE.

ANN NEUROL 2020;88:148–159

## Introduction

Anti-N-methyl-D-aspartate receptor encephalitis (NMDARE) is a well-characterized autoimmune encephalitis associated with IgG autoantibodies targeting the NR1 subunit of the NMDA glutamate receptor.<sup>1</sup> Symptoms include seizures, psychosis, memory loss, movement disorders, autonomic dysfunction, and decreased levels of consciousness. NMDARE represents one of the most common types of encephalitis,<sup>2,3</sup> and about 40% of all patients are children.<sup>4</sup> Similar to adult cases, routine magnetic resonance imaging (MRI) scans in pediatric NMDARE patients are often unremarkable, with unspecific MRI changes in about one-third of patients. These include transient T2 or fluid-attenuated inversion recovery (FLAIR) hyperintensities, contrast-enhancing abnormalities, or mild atrophy.<sup>5–7</sup> In adult patients, advanced neuroimaging studies revealed consistent structural and functional MRI changes, including hippocampal atrophy, white matter damage, and functional connectivity changes.<sup>8–11</sup> In contrast, there has been no systematic investigation of cerebral MRI changes in pediatric NMDARE so far. Here, we aimed to (1) evaluate structural MRI changes in a European cohort of 38 children with NMDARE and (2) identify potential imaging biomarkers for disease course and outcome. We longitudinally assessed MRI changes, performed volumetric MRI analysis with

age-optimized patient matching to a large cohort of healthy children, and used mixed-effect models and  $z$  score transformation for longitudinal analyses of brain volume changes. In addition, clinical presentation, diagnostic workup, and disease course were assessed, and disease severity as well as clinical outcome were correlated with clinical and MRI variables using ordinal logistic regression and mixed models.

## Subjects and Methods

### Patients

Patients were recruited from 13 European hospitals (Charité-Universitätsmedizin Berlin, Berlin, Germany; University Medical Center Hamburg-Eppendorf, Hamburg, Germany; Astrid Lindgren Children's Hospital, Karolinska University Hospital, Stockholm, Sweden; University Children's Hospital Augsburg, Augsburg, Germany; Medical University of Vienna, Vienna, Austria; Medical University of Innsbruck, Innsbruck, Austria; Dr von Hauner's Children's Hospital, Ludwig Maximilian University of Munich, Munich, Germany; Olgahospital, Stuttgart, Germany; Witten/Herdecke University, Datteln, Germany; Children's Hospital Neuburg, Neuburg, Germany; Marienhospital Bottrop, Bottrop, Germany; Gottfried von Preyer's Children's Hospital, Vienna, Austria; and Medical University Münster, Münster, Germany). All caregivers gave written informed consent. The study was approved by local ethics committees.

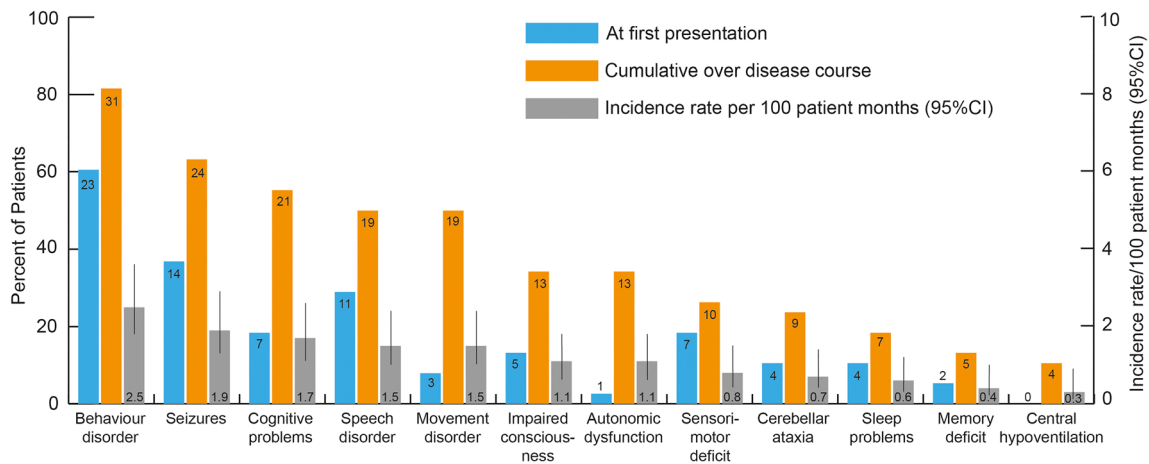


**FIGURE 1: Patient symptoms.** Patient symptoms at first presentation and over the disease course are given as number of patients (number written at the top or within the bar) and in percent (left y-axis). Incidence rate per 100 patient-months (right y-axis) is shown with error bars indicating the 95% confidence interval (CI). [Color figure can be viewed at [www.annalsofneurology.org](http://www.annalsofneurology.org)]

A total of 38 children with NMDARE were included (median age at disease onset = 12.9 years, range = 1–18, 31 [81.6%] female). Anti-NMDAR antibodies were confirmed in all patients in serum and/or cerebrospinal fluid (CSF) by commercially available assays. Clinical features and disease courses were retrospectively obtained from patient charts, and parameters such as age at onset, sex, presenting signs and symptoms, prior medical history, NMDAR antibody titer, CSF, electroencephalogram, routine MRI findings, treatment, clinical course, and outcome were collected for all patients and are presented in Table S1 and Figure 1. Median time for clinical follow-up was 35 months (range = 12–87 months). Disease severity and clinical outcome were assessed using the Pediatric Cerebral Performance Category (PCPC) scale.<sup>12</sup>

### Healthy Controls

MRI data from healthy children provided by the NIH MRI Study of Normal Brain Development were obtained via the Pediatric MRI Data Repository.<sup>13</sup> Briefly, this multicenter study includes serial MRI scans from >500 children, ranging from infants to young adults. For our analysis, we included a total of 1285 T1-weighted (T1w) MRI scans from 521 healthy children.

### Routine MRI Analysis

A total of 102 routine MRI scans (median scans per patient = 2, range = 1–6) of 38 patients were systematically reviewed to identify MRI abnormalities. Examples include T2/FLAIR hyperintensities, gray/white matter lesions, meningeal enhancement, and global/regional brain volume loss.

### Volumetric MRI Analysis

A total of 82 T1w MRI scans from 35 patients (median time to first MRI scan = 6 days, range = 0–585 days) were included for brain volume analysis. To allow reliable automated volumetric analysis, exclusion criteria for available MRI scans included persistent MRI lesions after herpes simplex virus (HSV) encephalitis (n = 3 patients, 10 MRI scans), extensive lesions associated with NMDARE (6 scans), and poor image quality (4 scans), for example movement artifacts. Volumetric analysis was performed using Functional Magnetic Resonance Imaging of the Brain Software Library (FSL) SIENAX and FSL FIRST. FSL SIENAX uses tissue-type segmentation estimating normalized whole brain, gray matter, white matter, cortical gray matter, and ventricular CSF volumes.<sup>14,15</sup> Volumes of subcortical structures were analyzed with FSL FIRST and normalized to head size using the *v*-scaling factor computed by SIENAX.<sup>16</sup>

### Group Comparison

Patient's brain volumes were first compared to age- and sex-matched healthy controls (1:10) in a cross-sectional group comparison using the *MatchIt* package for R,<sup>17</sup> that is, brain volumes obtained from 82 patient MRI scans were compared to brain volumes of 820 matched control MRI scans (patients vs controls, mean age in years ± standard deviation [SD]: 11.44 ± 5.95 vs 10.55 ± 5.87, *p* = 0.193; female patients: 71/82 [86.6%] vs 659/820 [80.4%], *p* = 0.187).

### Longitudinal Mixed-Effect Model (Brain Volume)

To account for individual differences in brain development in the pediatric population and the repeated-measure design, we applied longitudinal mixed-effect models to estimate individual longitudinal brain volume trajectories. Mixed-effect models in pediatric brain volume analysis account for intraindividual correlations and a heterogeneous number of measurements per subject in longitudinal observations.<sup>18</sup> The model was created using the *nlme* package for R.<sup>19</sup> Fixed effects included group (patients vs controls), age, time (time from disease onset or first MRI [for controls]), and sex as well as polynomial order age effects. Random effects included random intercepts accounting for varying interindividual baseline brain volumes and random slopes with brain volume development varying between subjects over time. Parameters were added using a forward selection mode, that is, starting with a simpler model and gradually including more parameters. The Akaike information criterion (AIC) was applied to compare the resulting models against each other and select the one with the best relative model quality. In general, lower AIC values represent better model quality in terms of goodness of fit while also penalizing model complexity due to the number of parameters.<sup>20</sup> As such, we selected the model with the lowest AIC value, which in turn resulted in choosing the simplest model with no further significant improvement in the log-likelihood ratio. Sample size correction was not warranted due to a favorable sample-to-parameter ratio. Including age in the model variables resulted in significant model improvement when considered as polynomial effects up to the third order (age<sup>3</sup>) but not beyond, such that higher-order polynomial age effects were discarded.

### Z Score Transformation

To additionally estimate patient brain volume changes from onset over the disease course, *z* scores were calculated for each patient MRI scan. This allowed for detection of brain volume differences of a patient MRI scan compared to its individually matched healthy control group of the same sex and age range. *Z* score transformation of the patient brain volume was calculated with the following formula:  $Z = \frac{v - \mu}{\sigma}$ , where *Z* is the patient brain volume *z* score, *v* is the measured patient brain volume, and  $\mu$  and  $\sigma$  correspond to the mean and SD of the individual normative control group. Age- and sex-matched controls were selected using the *MatchIt* package for R.<sup>17,21</sup> Our aim was to apply as many controls as possible while permitting biologically plausible comparability of a patient's brain volume to its expected healthy control group. To obtain the best-fitting age range of the respective control group for each patient MRI, we applied a data-driven age-matching optimization procedure, which specifies a maximum permitted age deviation of the matched controls from the patient age at MRI acquisition. The tradeoff between increasing the number of matched controls and restricting the maximum deviation from the patient age is linked to the finding that the age distribution in the NIH cohort is not uniform. As such, more control data are available for some ages (eg, 10 years old) than for others (eg, 4 years old). We therefore applied a minimum number (n = 5) of control scans and

determined the maximum number of matches by quality classification, where further matches were added until a specific quality cutoff was met. Matching quality was categorized into cutoffs at <2%, <5%, <10%, or <15% age deviation in days, depending on available data. Strict gender-matching was enforced for all patient MRIs. This approach allowed for age-adjusted matching with a stricter age-matching range in younger and a more liberal range in older children, reflecting the more dynamic brain development in younger compared to older children. Overall, matching quality based on this approach was very good, with the vast majority of control scans (>80%) adhering to <2% age deviation from patient age. For each patient MRI scan, the median number of matches was 16.5 (range = 5–25) and the median percent-age age deviation in days was 0.64% (range = 0.17%–11.93%).

### Incidence Rate (Ratios)

Incidence rates with 95% confidence intervals (CIs) were calculated for symptoms, PCPC scores, and MRI changes occurring over the disease course accounting for variable follow-up time. Incidence rate ratios (IRRs) were calculated comparing incidence rates for PCPC scores between groups (eg, patients with normal vs abnormal initial MRI).

### Ordinal Logistic Regression and Ordinal Logistic Mixed-Effects Models (Clinical)

Ordinal logistic regression models were used to predict clinical outcome (PCPC score at follow-up) and disease severity (maximum PCPC score). This approach allows for prediction of an ordinal scale (such as the PCPC scale) from continuous and/or categorical variables. All models were corrected for time from onset accounting for variable follow-up. Age at onset and gender were included (forced entry) to control for these factors.

An additional ordinal logistic mixed-effects model was built to predict PCPC score using all clinical follow-up data from a total of 272 patient visits. Models were built using the *clmm* function as part of the *ordinal* package for R. Predictors included time (logarithmic), age at onset, gender, MRI at onset, and brain volume z score as fixed effects, and subjects as random effects. Model building and selection were performed as described above for the brain volume longitudinal mixed-effect model (see above).

### Statistical Analysis

The Shapiro–Wilk test revealed non-normal distribution of all brain volume parameters. Therefore, volumetric group

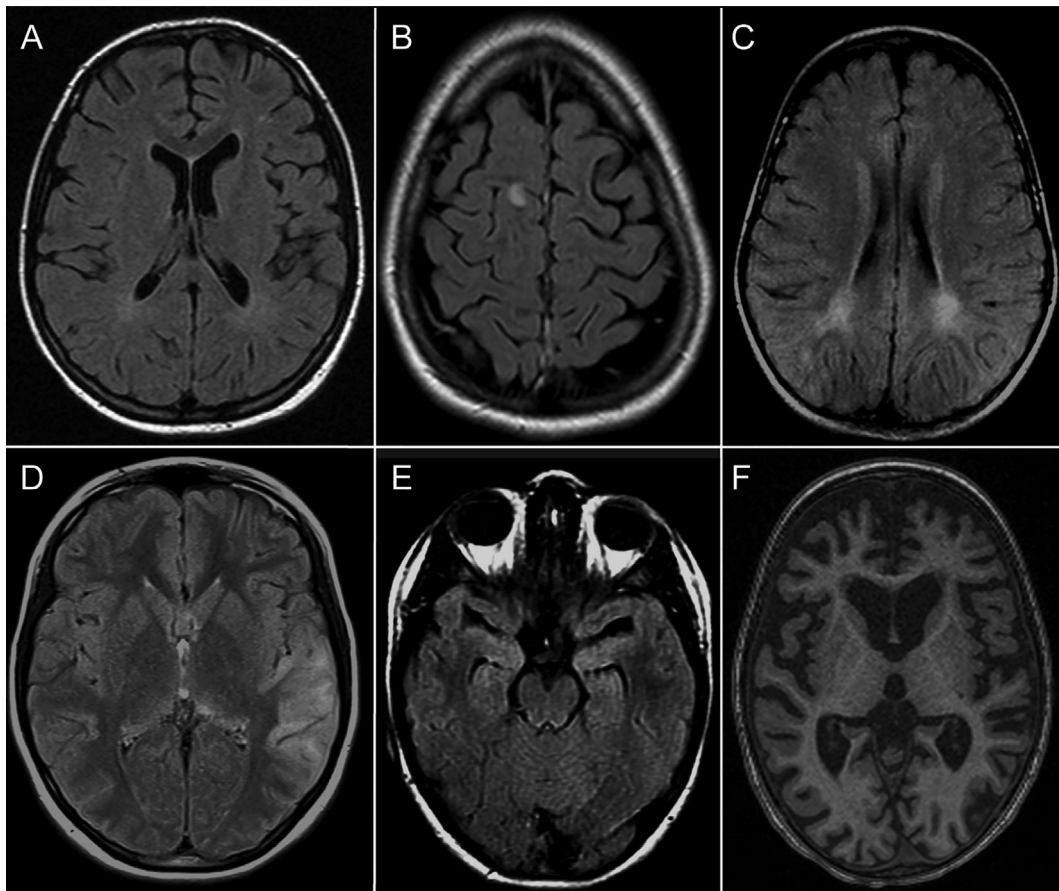


**FIGURE 2:** Clinical routine MRI scans in pediatric anti-N-methyl-D-aspartate receptor encephalitis (NMDARE). Examples are shown of abnormal findings in routine MRI scans of pediatric NMDARE patients. (A) Small punctuate white matter lesion in the left frontal lobe on fluid-attenuated inversion recovery (FLAIR) image. (B) Right frontal FLAIR lesion. (C) Bilateral white matter FLAIR signal alterations around the posterior horns of the lateral ventricles. (D) Cortical signal alteration of the left parietal lobe in FLAIR sequence. (E) Bilateral FLAIR hyperintensities in the medial temporal lobes, including both hippocampal formations. (F) Marked global atrophy in T1 sequence (cf Fig 3A for brain volume change over time).

differences were analyzed using the nonparametric Wilcoxon rank sum test (equivalent to Mann–Whitney test). Group differences in categorical data were analyzed using Pearson chi-square test or Fisher exact test, as appropriate. A point-biserial correlation was run to determine relationships between binary and continuous variables. Spearman coefficients were calculated for

correlation analyses between 2 continuous variables. All statistical tests were 2-sided, and  $p$  values  $< 0.05$  were considered significant. Multiple comparison correction was eschewed due to the explorative study design and to formulate new hypotheses and identify new prognostic factors. Analyses were implemented with custom-written code in R (v3.4.2 for Windows).

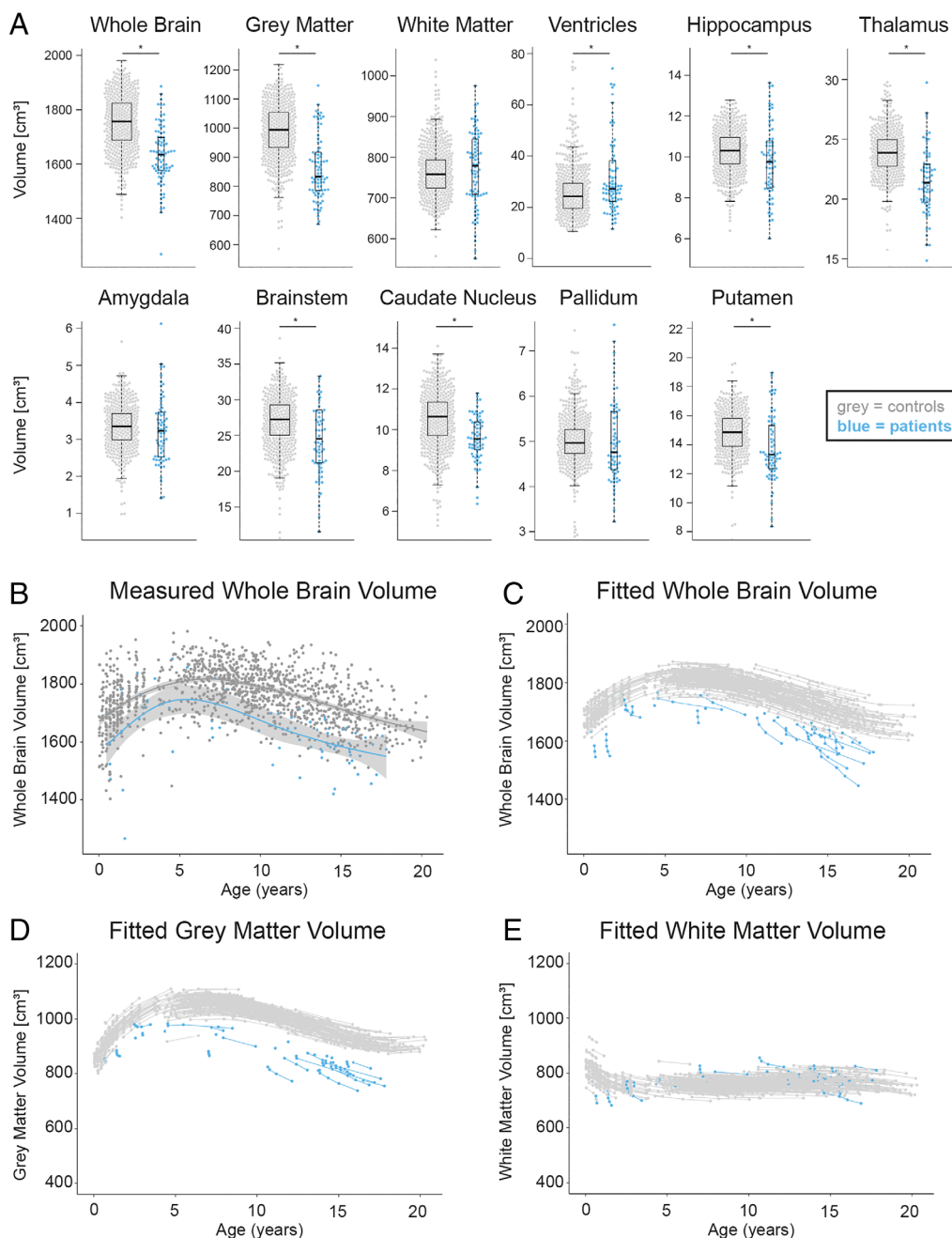


**FIGURE 3:** Brain volume loss and failure of age-expected brain growth in pediatric anti-N-methyl-D-aspartate receptor encephalitis (NMDARE) patients. (A) Group comparisons between patients and age- and sex-matched healthy controls (1:10) for whole brain, gray matter, white matter, ventricular, and subcortical volumes (box plots). Asterisks mark significant differences ( $p < 0.05$ ). (B) Normalized whole brain volume of NMDARE patients and healthy controls by age (in years). Each point represents 1 magnetic resonance imaging (MRI) scan; the 2 lines represent local polynomial regression fitting (locally estimated scatterplot smoothing) means with 95% confidence intervals for patients and controls. (C) Longitudinal mixed-effect model of whole brain volume over time. Note the different trajectories, with each line (representing 1 individual patient) connecting single points (representing single MRI scans) over time. (D, E) Longitudinal mixed-effect model of gray matter (D) and white matter (E) volume over time. Lines connect sequential MRI scans from 1 individual subject. [Color figure can be viewed at [www.annalsofneurology.org](http://www.annalsofneurology.org)]

**TABLE. 1. Volumetric Magnetic Resonance Imaging Analysis Group Comparison**

Area	Median Volumes, cm <sup>3</sup> (IQR)		W <sup>a</sup>	p
	Patients	Controls		
Whole brain	1,634.4 (122.1)	1,756.6 (136.4)	54,197	2.2e-16
Gray matter	833.5 (129.5)	994.1 (120.4)	54,881	2.2e-16
White matter	779.1 (133.9)	758.0 (68.8)	30,964	0.238
Ventricular CSF	27.2 (15.7)	24.3 (9.6)	25,648	3.9e-4
Subcortical				
Thalamus	21.4 (3.2)	23.9 (2.3)	36,880	5.1e-14
Putamen	13.3 (3.0)	14.9 (1.9)	32,601	4.1e-07
Caudate nucleus	9.6 (1.3)	10.7 (1.7)	33,816	8.2e-09
Pallidum	4.8 (1.3)	5.0 (0.5)	26,938	0.071
Hippocampus	9.7 (2.3)	10.3 (1.3)	28,752	0.004
Amygdala	3.2 (1.2)	3.4 (0.7)	26,476	0.124
Brainstem	24.5 (7.4)	27.3 (4.2)	29,098	0.002

<sup>a</sup>Wilcoxon rank sum test (equivalent to Mann–Whitney test).  
IQR = Interquartile range. CSF = Cerebrospinal fluid.

## Results

### Clinical Findings

Clinical details are shown in Table S1 and Figure 1. More than half (52.6% [20/38]) of patients fully recovered (PCPC = 1), whereas 47% showed mild/moderate (PCPC = 2–3: 21% [8/38]) to severe (PCPC = 4–6: 5.2% [2/38]) symptoms on follow-up after a median of 35 months (range = 12–87 months; see Table S1).

### Morphological MRI Changes

Routine MRI at disease onset showed abnormal findings in 15 of 38 (39.5%) children with NMDARE. These findings included small frontal or frontoparietal white matter T2/FLAIR hyperintense lesions (<3mm), more extensive white matter T2/FLAIR hyperintensities, cortical lesions, and hippocampal and thalamic signal alterations as well as focal (eg, hippocampal) and/or global atrophy (Fig 2). MRI changes at any time point during the disease course were found in 20 of 38 (52.6%) children with an incidence rate of 1.6 (95% CI = 1.0–2.5) per 100 patient months, including T2/FLAIR hyperintensities in brainstem, cerebellum, and frontal, parietal, and occipital lobes as well as infra- and supratentorial atrophy (see Fig 2F, Table S1). Three patients showed large temporal T2/FLAIR lesions characteristic of HSV encephalitis and were excluded from further volumetric MRI analysis.

### Volumetric MRI Analysis

Volumetric MRI analysis revealed whole brain atrophy at all ages (Fig 3B). A group comparison between patients and age- and sex-matched healthy controls (1:10) showed significantly reduced volumes of whole brain and gray matter in patients, whereas white matter volume was not significantly different between groups (Table and Fig 3A). Correspondingly, ventricular volume was significantly larger in patients compared to controls. Subcortical volumetric analysis showed significantly reduced volumes of the hippocampus, thalamus, putamen, caudate nucleus, and brainstem, but not amygdala and pallidum in patients.

Figure 3C illustrates the fitted longitudinal whole brain volume trajectories for individual patients and controls, showing a persistently reduced and declining brain volume in patients over the disease course. The optimal longitudinal mixed-effect model included third-order age, group (patients vs controls), and group\*time interaction as fixed effects, subjects as a random intercept, and age in subjects as random slope. Importantly, group (patients = 1 and controls = 0; estimated effect = -62.1, 95% CI = -96.5 to -27.8,  $p = 4 \times 10^{-4}$ ) and the interaction of group and time (estimated effect = -20.1, 95% CI = -33.3 to -6.9,  $p = 0.003$ ) were significant predictors, indicating not only a significant group difference in brain volume, but also a failure of normal brain development over time (negative estimated effect indicating smaller

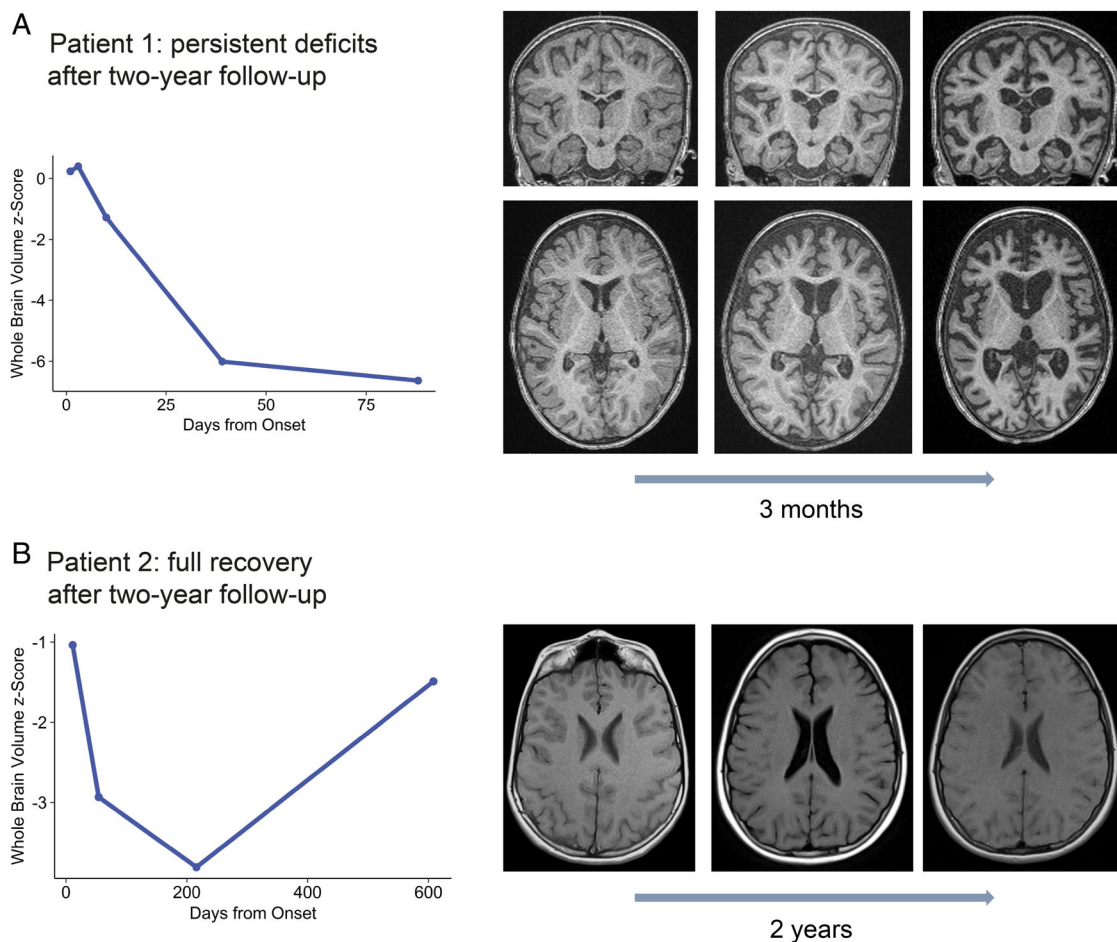


**FIGURE 4:** Case vignettes of 2 patients. (A) Progressive brain volume loss in a 2-year-old girl correlating with persistent deficits. After disease onset with prodromal fever and seizures, the girl developed reduced level of consciousness, sleep problems, dyskinesia, seizures, and agitation. Treatment included steroids, intravenous immunoglobulin (IVIG), plasma exchange, rituximab, and cyclophosphamide. At 2-year follow-up, severe intellectual and physical disability remained. Serum antibody titer at onset was 1:8,000, at 1 month was 1:100, at 2 months was 1:100, at 3 months was 1:320, at 1 year was 1:500, and at 2 years was negative. (B) Reversible brain volume loss correlating with full recovery in an 11-year-old girl. The patient presented initially with aggressive behavior and then developed reduced levels of consciousness, hallucinations, aphasia, seizures, and abnormal hand movements. She was treated with IVIG. At 2-year follow-up, she had a full recovery and was back at school. Serum antibody titer at onset was 1:100, at 1 month was 1:10, and at 3 months was negative. [Color figure can be viewed at [www.annalsofneurology.org](http://www.annalsofneurology.org)]

brain volume in patients vs controls) in patients compared to controls. Similarly, gray matter volume models suggest reduced volumes (estimated effect =  $-82.3$ , 95% CI =  $-114.5$  to  $-50.0$ ,  $p < 0.001$ ) and failure of age-expected gray matter development over time (estimated effect =  $-13.4$ , 95% CI =  $-25.8$  to  $-1.0$ ,  $p = 0.04$ ) in patients compared to controls, whereas white matter volume did not differ between patients and controls (estimated effect =  $17.1$ , 95% CI =  $-10.0$  to  $44.3$ ,  $p = 0.22$  and estimated effect =  $-6.2$ , 95% CI =  $-16.5$  to  $4.2$ ,  $p = 0.25$ ; see Fig 3D, E).

Z score transformation of each patient MRI allowed brain volume analysis with respect to disease onset for each individual patient (Fig 4). This analysis confirmed that patient brain volumes were generally smaller than the age-expected

brain volume ( $z$  score = 0). Gray matter volume showed a similar volume reduction over 2 years, whereas patients' white matter showed no relevant volume change over the disease course.

### Brain Volume Loss Correlates with Clinical Outcome

Whole brain and hippocampal volume loss significantly correlated with follow-up PCPC scores (whole brain:  $\rho = -0.450$ , Spearman's  $S = 8673.3$ ,  $p = 0.009$ ; hippocampus:  $\rho = -0.421$ ,  $p = 0.015$ ). Accordingly, brain volume  $z$  scores of patients with persistent deficits were significantly smaller compared to patients with full recovery (median =  $-2.00$ , interquartile range [IQR] =  $2.21$  vs median  $-1.05$ , IQR =  $1.19$ , Wilcoxon's  $W = 199$ ,  $p = 0.016$ ; Fig 5A). Similarly, hippocampus

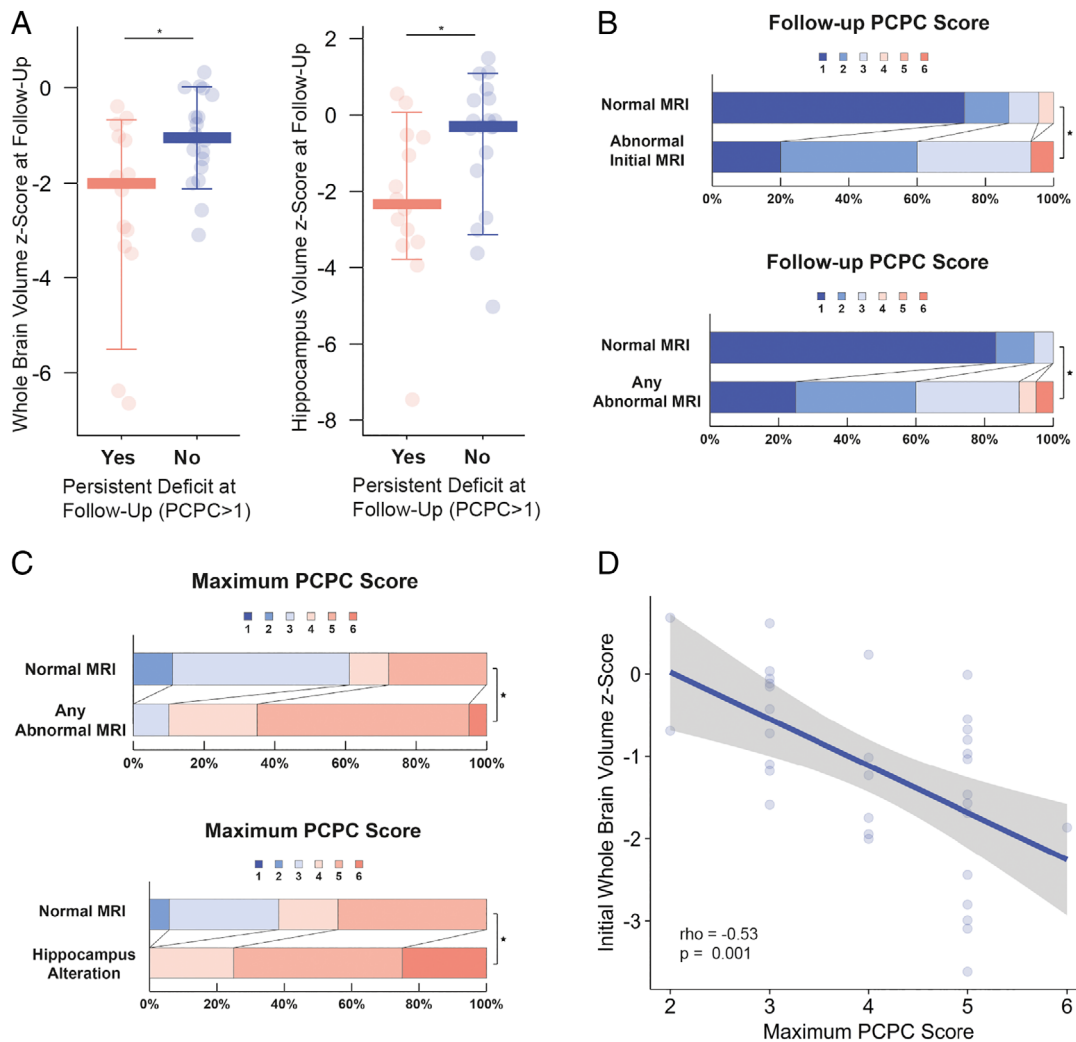


**FIGURE 5: Clinical routine magnetic resonance imaging (MRI) changes and brain volume loss predict disease severity and clinical outcome. (A, B) Clinical outcome. (A)** Patients with a persistent deficit (Pediatric Cerebral Performance Category [PCPC] > 1) display more brain (left) and hippocampus (right) volume loss (smaller whole brain volume and hippocampus volume z score at follow-up) compared to patients with full recovery. **(B)** Patients with an abnormal initial routine MRI (B, upper panel) or an abnormal MRI at any time (B, lower panel) exhibited poorer clinical outcome. Plot shows median and 10th to 90th quantile. Asterisks mark significant differences. **(C, D) Disease severity. (C)** Patients with an abnormal routine MRI at any time during disease course (C, upper panel), and MRI abnormalities in the hippocampus (C, lower panel) exhibit increased disease severity (maximum PCPC score). **(D)** Initial whole brain volume z score correlates with disease severity (maximum PCPC score); Spearman rho is shown (rho); line represents linear regression with 95% confidence interval. Asterisks mark significant differences throughout ( $p < 0.05$ ). [Color figure can be viewed at [www.annalsofneurology.org](http://www.annalsofneurology.org)]

z scores were smaller in patients with persistent deficits compared to patients with full recovery (median =  $-2.34$ , IQR = 2.55 vs median  $-0.30$ , IQR = 1.62,  $W = 198$ ,  $p = 0.017$ ). We did not find any correlations between different types of treatment and brain volume loss over time.

#### Clinical and MRI Predictors of Disease Outcome

Abnormalities on the initial routine MRI scan significantly correlated with clinical outcome, that is, PCPC score at follow-up (median = 2, IQR = 1.0 vs median = 1, IQR = 0.5,  $W = 80.5$ ,  $p = 0.003$ ; Pearson's point biserial

correlation  $r_{pb} = 0.430$ ,  $p = 0.007$ ; Fig 5B). Accordingly, patients with an abnormal initial routine MRI were significantly more likely to have persistent deficits (PCPC > 1 vs PCPC = 0: 80.0% [12/15] vs 26.1% [6/23], IRR = 3.5, 95% CI = 1.31–9.31,  $p = 0.012$ ). Abnormal MRI findings at any time across disease duration correlated even more strongly with clinical outcome (median = 2, IQR = 1.25 vs median = 1, IQR = 0,  $W = 69.5$ ,  $p = 0.001$ ;  $r_{pb} = 0.513$ ,  $p = 0.001$ ; see Fig 5B); a persistent deficit was found in only 3 patients with a normal routine MRI (eg, mild deficits in coordination and behavior) compared to 15 patients with abnormal MRI findings (16.7% [3/18] vs 75% [15/20], IRR = 5.4, 95% CI = 1.56–18.64,

$p = 0.008$ ). In addition, a sensory or motor deficit on initial neurological examination correlated with poor outcome (ie, PCPC score on clinical follow-up;  $r_{pb} = 0.451$ ,  $p = 0.004$ ); patients presenting with a sensorimotor deficit were at higher risk for a persistent deficit (IRR = 3.15, 95% CI = 1.12–8.83,  $p = 0.029$ ).

Furthermore, we analyzed whether clinical factors during the disease course correlated with disease outcome; in an exploratory analysis, there were significant correlations between sensorimotor deficits ( $r_{pb} = 0.41$ ,  $p = 0.011$ ) during the disease course as well as rituximab treatment ( $r_{pb} = 0.38$ ,  $p = 0.017$ ) with worse clinical outcome. However, applying IRR to account for observation time did not show significant correlations with clinical outcome. In addition, there was no correlation between age, gender, or antibody titer in serum or CSF with PCPC score at follow-up.

In an ordinal logistic regression model corrected for follow-up time, clinical outcome (PCPC score) was predicted by MRI and clinical variables; an abnormal routine MRI scan at onset (odds ratio [OR] = 9.90, 95% CI = 2.51–17.28,  $p = 0.009$ ), a clinical presentation with a sensorimotor deficit (OR = 13.71, 95% CI = 2.68–24.73,  $p = 0.015$ ), and a treatment delay > 4 weeks (OR = 5.15, 95% CI = 0.47–9.82,  $p = 0.031$ ) were independent significant predictors of a worse clinical outcome. Additional significant predictors in the model included brain volume  $z$  score (OR = -3.69, 95% CI = -6.65 to -0.72,  $p = 0.015$ ) and hippocampus volume  $z$  score (OR = -1.58, 95% CI = -2.74 to -0.41,  $p = 0.008$ ) at last follow-up. Other factors in the model included follow-up time, age at onset, gender, intensive care unit (ICU) admission, and CSF cell count > 20/ $\mu$ l (all not significant predictors).

An additional ordinal logistic mixed-effects model to account for the longitudinal data structure with variable follow-up time confirmed an abnormal initial MRI (OR = 7.06, 95% CI = 2.96–16.80,  $p = 0.001$ ) and last brain volume  $z$  score (OR = 0.64, 95% CI = 0.50–0.83,  $p = 0.001$ ) as significant predictors of the PCPC score. Other factors included (not significant) were follow-up time, age at onset, gender, and treatment delay > 4 weeks.

### **Clinical and MRI Predictors of Disease Severity**

Next, we analyzed whether routine MRI, volumetric MRI, or clinical parameters could predict disease severity as reflected by a patient's maximum PCPC score. Lower whole brain volumes on the initial MRI scan significantly correlated with a more severe disease course, that is, higher maximum PCPC scores ( $\rho = -0.531$ ,  $S = 9162.3$ ,  $p = 0.001$ ; see Fig 5D). In addition, presentation with cerebellar ataxia was associated with a more severe disease course (higher maximum PCPC score;  $r_{pb} = 0.670$ ,  $p = 0.013$ ). Furthermore,

MRI abnormalities at any time during the disease course correlated with higher disease severity (maximum PCPC in abnormal MRI vs normal MRI, median = 5, IQR = 1.0 vs median = 3, IQR = 1.75;  $W = 83$ ,  $p = 0.003$ ;  $r_{pb} = 0.511$ ,  $p = 0.001$ ), specifically when the hippocampus was affected (median = 5.0, IQR = 0.5 vs median = 4.0, IQR = 2.0;  $r_{pb} = 0.292$ ,  $p = 0.047$ ; see Fig 5C).

A second ordinal logistic regression model correcting for time from onset was built to predict disease severity. Here, a lower brain volume on the initial MRI ( $z$  score; OR = -1.90, 95% CI = -3.11 to -0.69,  $p = 0.002$ ), a clinical presentation with cerebellar ataxia (OR = 4.54, 95% CI = 0.19–8.88,  $p = 0.041$ ), and a hippocampus alteration on MRI (OR = 3.58, 95% CI = 0.48–6.69,  $p = 0.024$ ) were independent predictors of a more severe disease course (maximum PCPC score). Other factors included in the model were time from onset, age at onset, and gender (all not significant predictors).

### **Discussion**

We report the first systematic investigation of routine and advanced MRI analyses in pediatric NMDARE. MRI abnormalities were present in about 50% of NMDARE children. Children with abnormal MRIs exhibited a more severe disease course and a worse outcome compared to children with unremarkable MRIs. Longitudinal analyses revealed that children with NMDARE show significant brain volume loss over time and failure of age-expected brain growth that is driven by cortical and subcortical gray matter loss when compared to healthy controls. Importantly, abnormal findings (eg, T2/FLAIR hyperintensities) in the initial MRI scan, a sensorimotor deficit at disease onset, and a treatment delay > 4 weeks correlated with poor clinical outcome. Furthermore, smaller brain volumes on the initial MRI correlated with higher disease severity. These neuroradiological measures and clinical features may thus become clinically relevant biomarkers for disease course and outcome in children with NMDARE.

### **Routine MRI Abnormalities**

Around 40% of all patients with NMDARE are younger than 18 years. Although disease characteristics in children are generally similar to adult cases, there are important differences in clinical presentation, such as a higher prevalence of movement disorders, cerebellar ataxia, and sensorimotor deficits in children.<sup>4</sup> In contrast to these severe neurological symptoms, more than half of all patients have normal routine MRI scans throughout their disease course. In our study, routine MRI scans were abnormal in 40% of patients on initial MRI and in 50% across the disease course. Similarly, studies in adults reported normal MRIs in >50% of patients with abnormalities mainly including

subtle T2/FLAIR hyperintensities in the hippocampus, basal ganglia, brainstem, white matter, and cerebellar or cerebral cortex in frontobasal or insular regions.<sup>1,10,22–24</sup> In children, abnormalities on routine MRI were found in 31 to 45% of patients.<sup>5–7</sup> Whereas these previous studies suggested a slightly lower frequency of MRI abnormalities in children compared to adults,<sup>25</sup> our data indicate a similar prevalence. Abnormal MRI findings identified in our study included cortical, white matter, hippocampal, and thalamic T2/FLAIR hyperintensities, as well as regional (eg, hippocampal) and global atrophy. These results confirm and extend previously described changes in case series of pediatric NMDARE MRI that reported T2/FLAIR hyperintensities, atrophy, sulcal abnormalities, and cortical, parenchymal, or leptomeningeal enhancement.<sup>5–7</sup>

### **Brain Atrophy and Failure of Age-Expected Brain Growth**

Using volumetric analyses and longitudinal mixed-effect models, we found that NMDARE had a severe impact on the developing brain of children, resulting in brain volume loss and failure of age-expected brain growth over time. This is an important difference to our previous volumetric MRI analyses in adult patients.<sup>8</sup> Further analyses of our pediatric patients revealed reduced cortical and deep gray matter volume with reduced volumes of hippocampus, thalamus, and basal ganglia. This is in line with findings from adult NMDARE patients that identified atrophy and impaired functional connectivity of the hippocampus that correlated with memory impairment.<sup>8,9</sup> Interestingly, recent studies showed that many children similarly suffer from significant cognitive impairment following NMDARE, suggesting that the hippocampal volume loss found in our study might associate with impaired cognitive recovery.<sup>26,27</sup> Future studies are therefore warranted to assess the relationship of MRI changes and persistent cognitive deficits in pediatric NMDARE.

The majority of NMDARE children had persistently reduced whole brain volumes over time (see Fig 4A), in contrast to the majority of adult patients, who do not exhibit whole brain volume loss after the acute disease stage.<sup>8</sup> However, individual brain volume trajectories in our study indicated reversible brain volume loss with return to age-expected brain volume in a few children (see Fig 4B). This is in line with reversible diffuse brain volume loss that has been reported in single adult cases with severe disease courses that all required mechanical ventilation and prolonged hospitalization.<sup>28</sup> It should be noted, however, that these reports relied on visual MRI evaluation and did not apply volumetric MRI analyses. In addition, most children with NMDARE in our study had only moderate disease severity and nevertheless showed

relevant brain volume loss and failure of age-expected brain growth. This might indicate a more harmful impact of NMDARE on the developing brain of children compared to the adult brain. Interestingly, a recent study in children with acute disseminated encephalomyelitis (ADEM)—which is rare in adults, but the most common cause of immune-mediated encephalitis in children before NMDARE—found that pediatric ADEM patients showed brain volume loss and failure of age-expected brain development,<sup>29</sup> similar to our findings in pediatric NMDARE. However, the long-lasting impact on the developing brain—especially the impact on functional outcome—remains unclear. To answer this, further prospective longitudinal studies with cognitive outcome measures are needed.

### **Clinical and MRI Predictors of Disease Outcome and Severity**

More than half of all patients in our study fully recovered without any persistent neurological deficit over a median clinical follow-up of 3 years. This is in line with previous studies that found substantial improvement or complete recovery in up to 75% of pediatric cases.<sup>4,5</sup> Patients with a persistent deficit had more severe brain volume loss compared to patients with full recovery, suggesting a functionally relevant effect of the observed brain atrophy and failure of age-expected brain growth.

To improve clinical outcome, it is of major clinical relevance to identify patients at risk for severe disease courses and persisting deficits as early as possible. This allows guiding individual treatment decisions, for example, escalation to second- and third-line therapies, and counseling families on expected disease trajectory.<sup>30</sup> Using logistic regression and mixed-effect models, we found that an abnormal routine MRI as well as sensorimotor deficits at disease onset correlate with a poor clinical outcome. A sensorimotor deficit was found in up to 20% at initial presentation and almost 30% over time in our study. Interestingly, focal sensorimotor deficits are more common in children than in adult patients.<sup>4</sup> Nevertheless, motor cortex dysfunction has also been demonstrated in adult NMDAR patients using functional connectivity MRI analyses and transcranial magnetic stimulation.<sup>11,31</sup> A recent study identified a score predicting 1-year functional status in patients with NMDARE: anti-NMDAR Encephalitis One-Year Functional Status score.<sup>30</sup> The score includes 5 variables: treatment delay > 4 weeks, ICU admission, lack of clinical improvement within 4 weeks, abnormal MRI, and CSF white blood cell count > 20 cells/ $\mu$ l. In our study, we could replicate the finding of a treatment delay > 4 weeks and an abnormal MRI as predictors of worse clinical outcome. Importantly, we found that an

abnormal MRI already at first presentation (vs at any time during disease) was a significant independent predictor of worse clinical outcome. ICU admission and CSF white blood cell count > 20 cells/ $\mu$ l were not significant predictors in our data. This study, therefore, complements previous reports potentially identifying additional clinical predictors specifically for pediatric patients.

Although predicting disease outcome is the most relevant clinical variable, predicting severity of a patient's clinical course can also be helpful for (1) counseling of patients and parents on the expected disease trajectory and severity, (2) the decision process for early treatment and treatment escalation for more severely affected patients, and (3) inclusion of these parameters in clinical models for future prospective studies.

Smaller brain volume on initial MRI correlated with a more severe disease course. This suggests that the biological onset of NMDARE in children might precede the clinical presentation, resulting in brain volume loss already present on the initial MRI. Similar observations, that is, reduced brain volumes already at disease onset, have also been reported in children with multiple sclerosis.<sup>18,32</sup>

Limitations of the study include the retrospective study design, the relatively small sample size, especially in some of the subgroup analyses, and the lack of neuropsychological data. As this study aimed at exploring new clinical predictors, multiple comparison was not applied. Further studies are needed to replicate the findings from this study in larger and more diverse cohorts, applying a prospective design with standardized follow-up intervals and including cognitive measures accounting more accurately for long-term outcome associated with MRI volume changes.

In summary, our study is the first to systematically investigate cerebral MRI changes and volumetric MRI analyses in pediatric NMDARE. Children with NMDARE show substantial brain volume loss that is driven by cortical and subcortical gray matter loss as well as failure of age-expected brain development. Abnormal MRI findings at onset, a presentation with a sensorimotor deficit, and a treatment delay > 4 weeks correlate with poor clinical outcome, and initial brain volume loss correlates with a more severe disease course. Clinical routine MRI and brain volume changes thus represent promising biomarkers in pediatric NMDARE that should be validated in larger prospective studies.

## Acknowledgment

Funded by the Deutsche Forschungsgemeinschaft (DFG, German Research Foundation), grant numbers 327654276 (SFB 1315), FI 2309/1-1 (Heisenberg Program) and FI 2309/2-1; and the German Ministry of Education and

Research (BMBF), grant number 01GM1908D (CONNECT-GENERATE).

## Author Contributions

F.B., C.F., and K.R. contributed to conception and design of the study. All authors contributed to the acquisition and analysis of data. F.B., S.K., C.F., and K.R. contributed to drafting the text or preparing the figures.

## Potential Conflicts of Interest

Nothing to report.

## References

- Dalmau J, Gleichman AJ, Hughes EG, et al. Anti-NMDA-receptor encephalitis: case series and analysis of the effects of antibodies. *Lancet Neurol* 2008;7:1091–1098.
- Gable MS, Sheriff H, Dalmau J, et al. The frequency of autoimmune N-methyl-D-aspartate receptor encephalitis surpasses that of individual viral etiologies in young individuals enrolled in the California encephalitis project. *Clin Infect Dis* 2012;54:899–904.
- Granerod J, Ambrose HE, Davies NW, et al. Causes of encephalitis and differences in their clinical presentations in England: a multi-centre, population-based prospective study. *Lancet Infect Dis* 2010;10:835–844.
- Titulaer MJ, McCracken L, Gabilondo I, et al. Treatment and prognostic factors for long-term outcome in patients with anti-NMDA receptor encephalitis: an observational cohort study. *Lancet Neurol* 2013;12:157–165.
- Florance NR, Davis RL, Lam C, et al. Anti-N-methyl-D-aspartate receptor (NMDAR) encephalitis in children and adolescents. *Ann Neurol* 2009;66:11–18.
- Wright S, Hacoen Y, Jacobson L, et al. N-methyl-D-aspartate receptor antibody-mediated neurological disease: results of a UK-based surveillance study in children. *Arch Dis Child* 2015;100:521–526.
- Armangue T, Titulaer MJ, Málaga I, et al. Pediatric anti-N-methyl-D-aspartate receptor encephalitis—clinical analysis and novel findings in a series of 20 patients. *J Pediatr* 2013;162:850–856.e2.
- Finke C, Kopp UA, Scheel M, et al. Functional and structural brain changes in anti-N-methyl-D-aspartate receptor encephalitis. *Ann Neurol* 2013;74:284–296.
- Finke C, Kopp UA, Pajkert A, et al. Structural hippocampal damage following anti-N-methyl-D-aspartate receptor encephalitis. *Biol Psychiatry* 2016;79:727–734.
- Heine J, Prüss H, Bartsch T, et al. Imaging of autoimmune encephalitis—relevance for clinical practice and hippocampal function. *Neuroscience* 2015;309:68–83.
- Peer M, Prüss H, Ben-Dayana I, et al. Functional connectivity of large-scale brain networks in patients with anti-NMDA receptor encephalitis: an observational study. *Lancet Psychiatry* 2017;4:768–774.
- Fiser DH. Assessing the outcome of pediatric intensive care. *J Pediatr* 1992;121:68–74.
- Evans AC. The NIH MRI study of normal brain development. *Neuroimage* 2006;30:184–202.
- Smith SM, Zhang Y, Jenkinson M, et al. Accurate, robust, and automated longitudinal and cross-sectional brain change analysis. *Neuroimage* 2002;17:479–489.
- Smith SM, Jenkinson M, Woolrich MW, et al. Advances in functional and structural MR image analysis and implementation as FSL. *Neuroimage* 2004;23:S208–S219.

16. Patenaude B, Smith SM, Kennedy DN, Jenkinson M. A Bayesian model of shape and appearance for subcortical brain segmentation. *Neuroimage* 2011;56:907–922.
17. Ho DE, Imai K, King G, Stuart EA. MatchIt: nonparametric preprocessing for parametric causal inference. *J Stat Softw* 2011;42: 1–28.
18. Aubert-Broche B, Fonov V, Narayanan S, et al. Onset of multiple sclerosis before adulthood leads to failure of age-expected brain growth. *Neurology* 2014;83:2140–2146.
19. Pinheiro J, Bates D, DebRoy S, et al. Linear and nonlinear mixed effects models. R package nlme version 3.1–128. Vienna, Austria: R Foundation, 2016.
20. Akaike H. A new look at the statistical model identification. *IEEE Trans Automat Control* 1974;19:716–723.
21. Ho DE, Imai K, King G, Stuart EA. Matching as nonparametric preprocessing for reducing model dependence in parametric causal inference. *Polit Anal* 2007;15:199–236.
22. Irani SR, Bera K, Waters P, et al. N-methyl-D-aspartate antibody encephalitis: temporal progression of clinical and paraclinical observations in a predominantly non-paraneoplastic disorder of both sexes. *Brain* 2010;133:1655–1667.
23. Dalmau J, Tüzün E, Wu HY, et al. Paraneoplastic anti-N-methyl-D-aspartate receptor encephalitis associated with ovarian teratoma. *Ann Neurol* 2007;61:25–36.
24. Bacchi S, Franke K, Wewegama D, et al. Magnetic resonance imaging and positron emission tomography in anti-NMDA receptor encephalitis: a systematic review. *J Clin Neurosci* 2018;52:54–59.
25. Sweeney M. Autoimmune neurologic diseases in children. *Semin Neurol* 2018;38:355–370.
26. De Bruijn MAAM, Aarsen FK, Van Oosterhout MP, et al. Long-term neuropsychological outcome following pediatric anti-NMDAR encephalitis. *Neurology* 2018;90:e1997–e2005.
27. Matricardi S, Patrini M, Freri E, et al. Cognitive and neuropsychological evolution in children with anti-NMDAR encephalitis. *J Neurol* 2016;263:765–771.
28. Iizuka T, Kaneko J, Tominaga N, et al. Association of progressive cerebellar atrophy with long-term outcome in patients with anti-N-methyl-d-aspartate receptor encephalitis. *JAMA Neurol* 2016; 73:706–713.
29. Aubert-Broche B, Weier K, Longoni G, et al. Monophasic demyelination reduces brain growth in children. *Neurology* 2017;88: 1744–1750.
30. Balu R, McCracken L, Lancaster E, et al. A score that predicts 1-year functional status in patients with anti-NMDA receptor encephalitis. *Neurology* 2019;92:e244–e252.
31. Volz MS, Finke C, Harms L, et al. Altered paired associative stimulation-induced plasticity in NMDAR encephalitis. *Ann Clin Transl Neurol* 2016;3:101–113.
32. Bartels F, Nobis K, Cooper G, et al. Childhood multiple sclerosis is associated with reduced brain volumes at first clinical presentation and brain growth failure. *Mult Scler J* 2019;25: 927–936.